Peak Effect and the Phase Diagram of Moving Vortices in $Fe_xNi_{1-x}Zr_2$ Superconducting Glasses

M. Hilke,* S. Reid, R. Gagnon, and Z. Altounian
Department of Physics, McGill University, Montréal, Canada H3A 2T8
(Received 5 May 2003; published 18 September 2003)

In the mixed state of type II superconductors, vortices penetrate the sample and form a correlated system due to the screening of supercurrents around them. Interestingly, we can study this correlated system as a function of density and driving force. The density, for instance, is controlled by the magnetic field B, whereas a current density j acts as a driving force $F = j \times B$ on all vortices. To minimize the pinning strength, we study a superconducting glass in which the depinning current is 10 to 1000 times smaller than in previous studies, which enables us to map out the complete phase diagram in this new regime. The diagram is obtained as a function of B, driving current, and temperature, and leads to a remarkable set of new results, which includes a huge peak effect, an additional reentrant depinning phase, and a driving force induced pinning phase.

DOI: 10.1103/PhysRevLett.91.127004 PACS numbers: 74.25.Dw, 74.25.Op, 74.25.Qt, 74.25.Sv

The peak effect (PE), which is one of the most intriguing consequences of the motion of vortices in superconductors, is a peak in the critical current as a function of B. The PE typically occurs below, but near, the critical field (B_{c2}) in some strong type II conventional superconductors [1–5]. In high temperature superconductors, the PE is also observed but usually appears well below B_{c2} [6] as inferred from magnetotransport measurements. The PE can lead to a reentrant superconducting phase as a function of B or T when a current slightly below the maximum critical current is applied. Above the critical current, vortices experience a force strong enough to be depinned and they start moving, which leads to a nonzero electrical field ($E = \bar{v} \times B$) and, hence, to a nonzero resistance, where $\bar{v}$ is the average vortex velocity. At the PE, the vortices are pinned again, which decreases the resistance and enhances the critical current. While the exact mechanism of the PE is not fully understood, recent experiments on Nb have correlated the PE with the disappearance of neutron scattering Bragg peaks from the vortex structure. This was attributed to the transition from a long-range ordered phase to a short-ranged disordered phase, which in turn is pinned more efficiently [7,8]. This transition can be induced either by increasing disorder or equivalently by increasing B, since the disorder potential couples to all vortices, hence effectively increasing with B. However, recent experiments on $NbSe_2$ have questioned the amorphous nature of the phase in the PE regime [9].

In this work, we investigate the vortex dynamics in a system with the weakest possible pinning potential. It is well known that amorphous superconductors have a lower critical current than crystals because of the absence of long-range order, which implies weaker collective pinning. The remaining pinning is then mainly governed by impurities. We therefore used high purity Fe-Ni-Zr based superconducting glasses, which have a similar critical temperature (T_c) and B_{c2} as the widely studied crystalline 2H-$NbSe_2$ system [1] and others [3,4,6–9], but our amorphous samples exhibit a critical current density ($J_c \leq 0.4$ A/cm^2), just below the PEt, which is typically 100 to 1000 times smaller. In comparison to earlier studies on the PE in amorphous films, our samples still have a J_c 10 times smaller [2,5,10,11], which reflects the high level of purity of our samples.

We obtained these high purity superconducting glasses by melt spinning [12] $Fe_xNi_{1-x}Zr_2$ with different values of x. Although we only present results for $x = 0.3$, qualitatively very similar features were obtained for $x = 0$, 0.1, and 0.2, which suggests that these effects are inherent to these types of materials and do not depend critically on composition. In general, superconductivity in these systems is suppressed by spin fluctuations when increasing the Fe concentration further [13]. The transition temperature (T_c) for $x = 0.3$ is 2.30 ± 0.02 K as extracted from three different samples. The sharpness of the transition region is quite remarkable, with a transition temperature width (10%–90% value) ranging between 5 and 20 mK for all three samples, indicative of very homogenous samples. The absence of crystallinity is confirmed by the absence of Bragg peaks in x-ray diffraction. The samples have the following typical sizes (thickness = 21 μm, width = 1.15 mm, and length between indium contacts = 8 mm). Using standard expressions for superconductors in the dirty limit [5], we can estimate the different length scales in our system. The zero temperature penetration depth is $\lambda = 1.05 \times 10^{-3}(\rho_N/T_C)^{1/2} \simeq 0.9$ μm, the BCS coherence length is $\xi \simeq 7.3$ nm [or 8.3 nm using Ginzburg-Landau (GL)], the GL parameter $\kappa \simeq 76$, and $B_{c1} \simeq 29$ mT. Relevant experimental quantities are $T_c = (2.30 \pm 0.02)$ K, $B_{c2}(T = 0) = (4.8 \pm 0.1)$ T, $\rho_N = (1.7 \pm 0.2)$ $\mu\Omega$ m (normal resistivity), and $[(dB_{c2})/(dT)]|_{T_c} = (-2.7 \pm 0.2)$ T/K. These numbers are typical for a strong type II low-T_c material.

Since moving vortices give rise to a nonzero resistance in a superconductor, we measured the B dependence of

the magnetoresistance for different currents to probe the dynamics of the vortices. The results are presented in Fig. 1. The most striking feature is the B-induced reentrant superconducting phase for currents above 0.07 mA. Such a strong reentrant superconductor was never observed before in any amorphous superconductor. However, because we observed a similarly strong reentrant behavior for different concentrations of Fe ($x = 0$, 0.1, and 0.2), we believe that this effect is very general for high purity and weakly pinned amorphous superconductors. Indeed, when comparing our results to previous studies on the PE in amorphous superconductors [2,5,10,11], the most notable difference is the critical current, which is a measure of the pinning strength and is at least 10 times smaller in our samples, indicating that weak pinning enhances the reentrant behavior. The reentrant behavior is the most dramatic signature of the PE, which disappears below 0.07 mA and implies a peak in the critical current in the region of the reentrant superconductor.

We map out the phase diagram of the moving vortices using the dissipative transport in Fig. 1 and illustrated by the top figure with the help of the 1 mA down-sweep curve. The results of the diagram are presented in Fig. 2. At low fields, we have the first depinning transition defined when the resistance exceeds 0.5 mΩ, which is our experimental resolution. The choice of this cutoff is not critical since close to the depinning transition the dependence of the resistance on B is stronger than exponential. When increasing B further, the system becomes more and more resistive for currents above 0.07 mA. In this region, which we denote depinning 1, the vortices start moving. At even higher B, the moving vortices are pinned again in the pinning region, which leads to the reentrant superconducting phase inside this pinning region. The pinning transition is defined when $dR/dB = 0$. Inside the pinning region, the resistance eventually vanishes within our experimental resolution (0.5 mΩ). Finally, at high enough B we cross B_{c2} and the system becomes normal. B_{c2} is defined as the point of strongest negative curvature just before reaching the normal state. At higher driving currents, we observe another region, labeled depinning 2, which corresponds to a sudden increase of resistance after the pinning or depinning 1 regions, indicative of another depinning transition, before reaching B_{c2}, which is defined as the point of highest positive curvature.

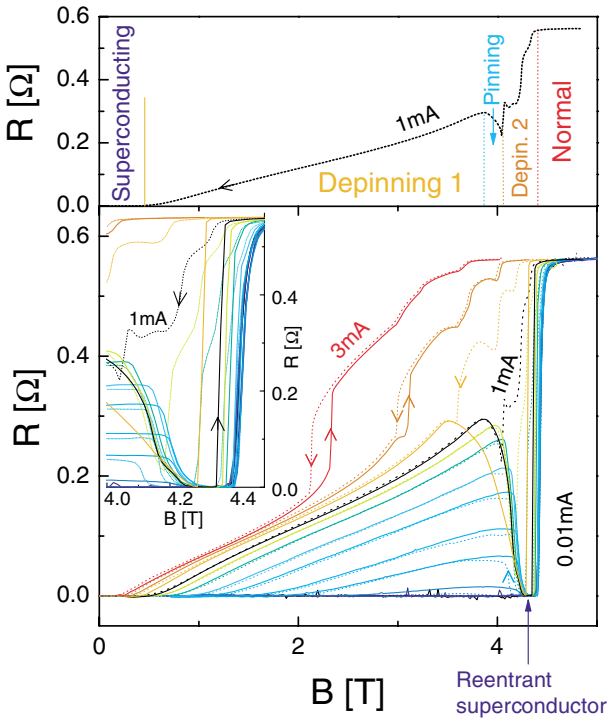

FIG. 1 (color online). Lower curves: Resistances as a function of B for up and down B sweeps. The left curves expand the high field region. The different curves are for different currents, ranging from 0.01 to 3 mA (0.01, 0.02, 0.04, 0.07, 0.1, 0.15, 0.2, 0.3, 0.4, 0.6, 0.8, 1.0, 1.5, 2.1, 3) mA. The upper curve, which is the resistance for the down sweep with 1 mA, illustrates how we determine the different transition points. The resistances were measured using an ac resistance bridge at 17 Hz and $T = 450$ mK.

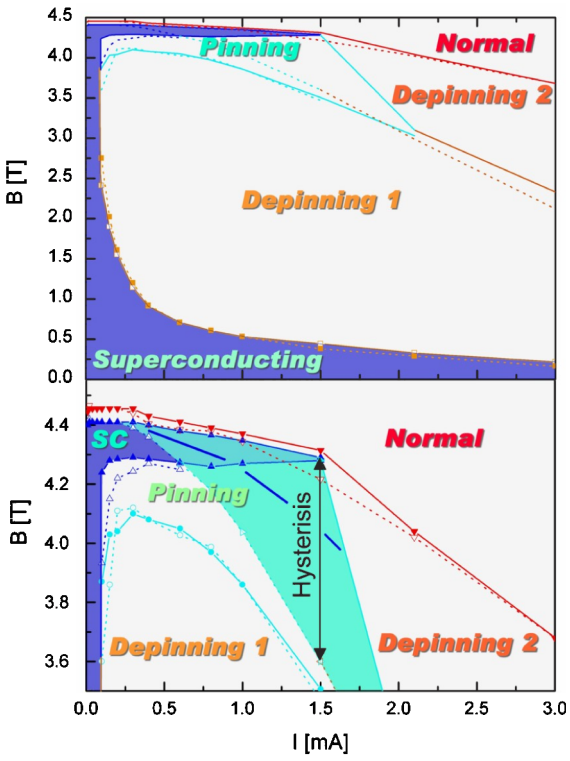

FIG. 2 (color online). Phase diagram of vortex dynamics as extracted from Fig. 1. The solid lines are obtained when sweeping B up and the dotted lines when B is swept down. The lower half is an enlargement of the high B region. Overall, the diagram is consistent with three distinct phases (depinning 1, pinning, and depinning 2) connected by a strongly hysteretic triple point at the end of the thick dashed line.

A striking feature of the phase diagram is the huge PE at 4.3 T. Indeed, the critical current, which delimits the superconductor (shaded in dark in Fig. 2) from the nonzero resistance depinned phases, jumps from 0.07 mA to 1.5 mA close to 4.3 T. This PE is associated with the depinning 1 to pinning transition of the vortices.

Quite generally, the depinning 1 region is characterized by weakly pinned vortices, which move beyond a B-dependent activated threshold. Giamarchi and coworkers [14] argued that this phase is a long-range ordered moving Bragg glass (MBG), consistent with a recent experiment showing algebraic neutron scattering Bragg peaks in this region with measurements performed on (K, Ba)BiO_3 [15]. Our results support this picture since the dependence of the voltage (V) on current (I) below the PE for B fields between 0.25 and 3.75 T (as illustrated in the inset of Fig. 3) is well fitted by the activated creep expression $V \sim e^{-U/T\sqrt{I}}$. This is in contrast to the region close to the PE, where we observe a negative differential resistance shown in the main part of the figure and discussed at the end. U reflects the pinning strength and the expression was derived directly from the equation of motion [16] and assumes a long-range ordered phase, such as a Bragg glass. The long-range nature of this phase can be inferred from the geometry dependent transition point; indeed, when tilting the field so that B is aligned along the wide axis of the sample (instead of perpendicular to it), the transition is shifted upwards between 1.5 and 2.5 T depending on the current. Since the sample is amorphous and 1 mm wide but only 20 μm thick, this implies long-range order above 20 μm. This transition is the only one, which is significantly affected by the tilted field below 1.5 mA, suggesting that the remaining phases have shorter ranged order.

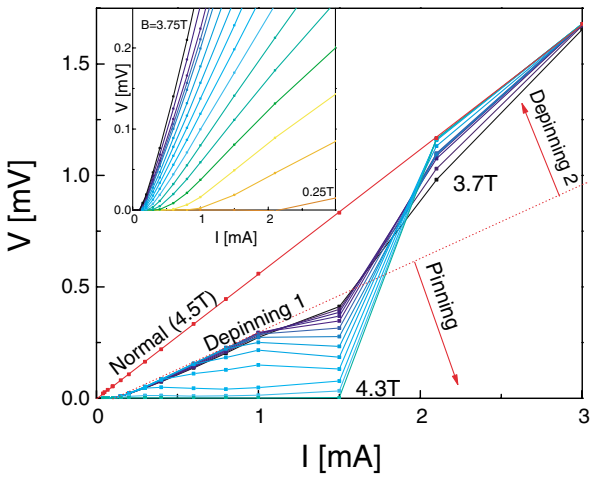

FIG. 3 (color online). Dependence of the voltage as a function of driving current for increasing field ($3.7 < B < 4.3$ T). Inset: Dependence of the voltage on driving current for decreasing field ($B < 3.7$ T).

At higher B, the pinning increases in the PE region. In this region the intervortex distance is close to ξ, which is the size of the vortex core and implies strong intervortex correlations. The exact nature of this pinning transition is still under debate, but it is commonly associated with an order-disorder transition [17], the melting of the vortex structure [18], or the anomalous friction close to B_{c2} [19]. Experimentally, the reentrant superconductor is nonetheless the most spectacular demonstration for the existence of a depinning to pinning transition. In Fig. 2, the reentrant superconductor is shaded in dark, which is included in the pinning region. We mapped out the pinning regions for both B-sweep directions up (solid lines) and down (dotted lines) and observed an increasing hysteresis as a function of driving current, which is the lightly shaded region. The region of hysteresis does not depend on the sweeping rate and is stable once reached. The left inset of Fig. 1 shows details of the region of hysteresis and the B-sweep direction is labeled with corresponding arrows. The hysteresis is particularly striking, when coming from the low B region into the pinning region. Indeed, at a fixed $B = 4.3$ T and $I = 1$ mA, the sample is superconducting, then we can either increase the current to 2 mA and back or sweep B to 4.5 T and back, or increase T to 1 K and back, and the sample is no longer superconducting and remains dissipative on time scales beyond our experiment. Sweeping B to 3.5 T and back recovers a highly stable superconducting phase. Hence, for the same B and I we can have two different phases, which are stable over very long time scales. Moreover, when increasing the temperature, the size of the region of hysteresis decreases and eventually vanishes as illustrated in Fig. 4 (the lightly shaded region). Since the dependence on temperature is noncritical, this transition is strongly suggestive of a first order phase transition inside the region of hysteresis, which we indicated as a thick dashed line in Fig. 2. This is in agreement with earlier experiments on crystals [20,21], but in our system this first order transition is not

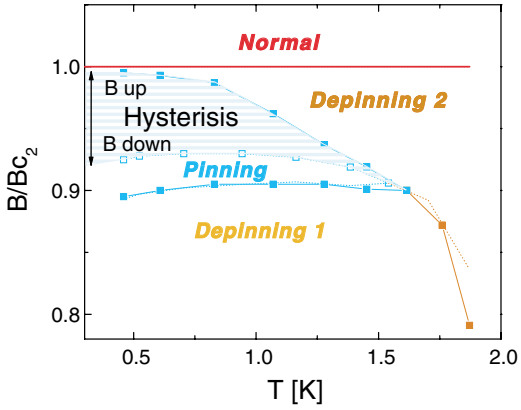

FIG. 4 (color online). Phase diagram as a function of temperature. The data was rescaled to Bc_2 and taken for B applied parallel to the wide axis of the sample with $I = 1$ mA.

associated with the formation of the pinning region but rather with the transition to the depinning 2 phase at B fields above the PE.

This additional depinning 2 phase between the PE and the normal phase is only seen at sufficiently high driving currents (Fig. 2) and is masked by the hysteresis at low T and becomes more apparent at higher T as seen in Fig. 4. This hints to a much richer transition region between the PE and the normal state than previously expected and constitutes an important new experimental finding for the theoretical understanding of these systems.

At even higher currents, the depinning 2 region can be reached directly from the depinning 1 region, which corresponds to a sudden delocalization of the vortices identified by a jump in the resistance. This region is not an inhomogeneous mix of normal and superconducting regions because at low currents the superconducting-to-normal transition is extremely sharp, i.e., less than 50 mT wide for the 10%–90%, which excludes any large scale inhomogeneities in the sample. This type of transition is consistent with several theoretical and numerical results [22–24] describing the transition from a MBG to a smectic or plastic flow of vortices. Moreover, the depinning 2 region is increasingly geometry dependent at large currents above 2 mA as observed from tilted field measurements, which suggests that the vortex order of the depinning 2 region increases with current as expected from the above-mentioned theoretical results.

However, there is an overall downward bending of the pinning region with current, which implies that for some fields vortices get pinned again before they eventually depin. This is very unusual and has never been observed before in the context of vortices. This behavior explains the negative differential resistance observed in Fig. 3 as a function of current for $B \simeq 4$ T, which implies a dynamical pinning mechanism at high average vortex velocities. This effect cannot be due to an increase of effective T since B_{c2} is almost not affected by currents in this range, but it is hysteretic and might be due to the nonmonotonous ordering as a function of driving force, similar to the situation of driven charge-density waves [25].

In summary, we have studied a new class of superconductors in relation to the peak effect, in which the depinning threshold is extremely weak and where there is no underlying crystalline order. In our system the PE is huge, with an increase by more than an order of magnitude of the critical current in the PE region, indicating that very low pinning tends to enhance the peak effect. In addition, after mapping out the entire phase diagram of our system, while many similarities with previous studies on the PE have been found, we also observed two striking differences. Indeed, we observed an additional transition between the PE and the normal state as well as a dynamical pinning transition at constant vortex density. These results have important implications on our understanding of the dynamics of vortices in very weakly pinned systems.

The authors would like to acknowledge helpful discussions with T. Ala-Nissila, M. Grant, H. Guo, S. Sondhi, and J. O. Strom-Olsen, and support from NSERC and FCAR.

*Electronic address: Hilke@physics.mcgill.ca

[1] M. J. Higgins and S. Bhattacharya, Physica (Amsterdam) **257C**, 232 (1996).
[2] T. G. Berlincourt, R. R. Hake, and D. H. Leslie, Phys. Rev. Lett. **6**, 671 (1961).
[3] E. S. Rosenblum, S. H. Autler, and K. H. Gooen, Rev. Mod. Phys. **36**, 77 (1964).
[4] A. B. Pippard, Philos. Mag. **19**, 217 (1969).
[5] P. H. Kes and C. C. Tsuei, Phys. Rev. B **28**, 5126 (1983).
[6] W. K. Kwok, J. A. Fendrich, C. J. van der Beek, and G.W. Crabtree, Phys. Rev. Lett. **73**, 2614 (1994).
[7] A. M. Troyanovski M. van Hecke, N. Saha, J. Aarts, and P. H. Kes, Phys. Rev. Lett. **89**, 147006 (2002).
[8] P. L. Gammel *et al.*, Phys. Rev. Lett. **80**, 833 (1998).
[9] Y. Fasano *et al.*, Phys. Rev. B **66**, 020512 (2002).
[10] J. M. E. Geers, C. Attanasio, M. B. S. Hesselberth, J. Aarts, and P. H. Kes, Phys. Rev. B **63**, 094511 (2001).
[11] R. Wördenweber, P. H. Kes, and C. C. Tsuei, Phys. Rev. B **33**, 3172 (1986).
[12] Z. Altounian, Tu Guo-hua, and J. O. Strom-Olsen, J. Appl. Phys. **53**, 4755 (1982).
[13] Z. Altounian and J. O. Strom-Olsen, Phys. Rev. B **27**, 4149 (1983).
[14] T. Giamarchi and P. Le Doussal, Phys. Rev. B **52**, 1242 (1995).
[15] T. Klein *et al.*, Nature (London) **413**, 404 (2001).
[16] P. Chauve, T. Giamarchi, and P. Le Doussal, Phys. Rev. B **62**, 6241 (2000).
[17] For recent reviews on vortex phases, see T. Giamarchi and S. Bhattacharya, in *High Magnetic Fields. Applications in Condensed Matter Physics and Spectroscopy*, edited by C. Berthier, L. P. Levy, and G. Martinez (Springer-Verlag, Berlin, 2001), p. 314.
[18] A. I. Larkin, M. C. Marchetti, and V. M. Vinokur, Phys. Rev. Lett. **75**, 2992 (1995).
[19] E. Granato, T. Ala-Nissila, and S. C. Ying, Phys. Rev. B **62**, 11 834 (2000).
[20] E. Zeldov *et al.*, Nature (London) **375**, 373 (1995).
[21] M. Marchesky, M. J. Higgins, and S. Bhattacharya, Nature (London) **409**, 591 (2001).
[22] T. Giamarchi and P. Le Doussal, Phys. Rev. B **57**, 11 356 (1998).
[23] C. J. Olson, C. Reichhardt, and Franco Nori, Phys. Rev. Lett. **81**, 3757 (1998).
[24] H. Fangohr, S. J. Cox, and P. A. J. de Groot, Phys. Rev. B, **64**, 064505 (2001).
[25] M. Karttunen, M. Haataja, K. R. Elder, and M. Grant, Phys. Rev. Lett. **83**, 3518 (1999).